Dispersion properties of the out-of-plane transverse wave in a two-dimensional Coulomb crystal

K. Qiao and T. W. Hyde*
CASPER (Center for Astrophysics, Space Physics, and Engineering Research), Baylor University, Waco, Texas 76798-7310, USA
(Received 8 May 2003; published 22 October 2003)

The formation of a two-dimensional (2D) Coulomb crystal in a typical experimental environment was simulated with a computer code called BOX_TREE. The dispersion properties of a novel dust lattice wave (DLW) mode, the *out-of-plane* transverse wave, were obtained. The dispersion relation was determined to be an opticlike inverse dispersion when wave number k is lower than a critical value k_{critical}, and a positive dispersion when $k>k_{\text{critical}}$. The negative group velocity of the wave for $k<k_{\text{critical}}$ depends on the κ value (with $\kappa=a/\lambda_D$, where a is the interparticle spacing and λ_D is the Debye length) and the positive group velocity for $k>k_{\text{critical}}$ depends on the propagation direction. The value of k_{critical} depends on both κ and propagation direction, but changes very little for all propagation directions and the range of κ investigated. An analytical method has also been used to derive the dispersion relations assuming a hexagonal 2D lattice and Yukawa interparticle potential. These dispersion relations compare favorably with the simulation results. The dispersion relation for a 1D string was also obtained via BOX_TREE simulation and shown to agree with the analytical result given by Vladimirov [Physica A **315**, 222 (2002)]. Comparison shows that the *out-of-plane* transverse DLW in a 2D lattice when $k<k_{\text{critical}}$ has a negative group velocity much larger than that of the 1D string, given the same particle parameters and operating environment. Again k_{critical} for 1D string and 2D lattice are in the same range.

DOI: 10.1103/PhysRevE.68.046403 PACS number(s): 52.35.Fp, 52.27.Lw, 52.27.Gr

I. INTRODUCTION

The two-dimensional (2D) Coulomb crystal produced in a typical laboratory complex (dusty) plasma environment is formed when dust particles are levitated in the sheath region of a rf discharge plasma [1–3]. Dust particles immersed in a plasma are usually negatively charged due to electron currents. Once charged, these particles are then levitated in a horizontal plane in the sheath region of the lower electrode due to a balance between gravity and the electrostatic force from the lower electrode. This system of particles is usually constrained on the horizontal direction by an inwardly directed electric field force. The negative charge on a particle is shielded by the ambient plasma resulting in the particles interacting with each other through a repulsive Yukawa potential defined by $V(r)=Q\exp(-r/\lambda_D)/4\pi\varepsilon_0 r$, where r is the distance between any two particles and λ_D is the dust Debye length. The dust particles constrained in the plane form a hexagonal lattice due to this potential and make a 2D Coulomb crystal.

Two types of dust lattice waves (DLW) in 2D Coulomb crystals have been studied both theoretically [6,9] and experimentally [4–8]. Both of these wave modes (the longitudinal and the *in-plane* transverse) involve motion of the particle in the horizontal plane [9]. However, it has recently been shown [10] that the dust particles can also move vertically out of the plane. This motion out of the plane leads to another low-frequency transverse dust lattice wave mode, which can be responsible for phase transitions in the system. An optic-mode-like inverse dispersion has been suggested for the vertical wave motion in a horizontal chain [10], however the detailed dispersion properties of this *out-of-plane* transverse wave in the 2D Coulomb crystal are not yet understood.

In this research, a numerical code called BOX_TREE was used to simulate the formation of a 2D Coulomb crystal under the balance of gravity and a linear electrostatic field. The dispersion relation of the *out-of-plane* DLW was obtained by analyzing the vertical motion of the particles in this Coulomb crystal. DLWs with various propagation directions and various shielding parameters κ (with $\kappa=a/\lambda_D$, where a is the interparticle spacing and λ_D is the Debye length) are discussed.

An analytical method is also employed to derive the *out-of-plane* transverse DLW dispersion relation assuming a 2D hexagonal Coulomb crystal formed under an external linear electrostatic force, gravity, and the interparticle Yukawa force. The simulation results are shown to agree with the analytical results.

Finally, a simulation was run for a 1D string of particles. The results were then compared with both the 2D lattice results and the Vladimirov analytical results as given in [10].

II. NUMERICAL METHOD

The BOX_TREE code is a Barnes-Hut tree code first written by Richardson [11] for planetary ring and disk studies. It was later modified by Matthews and Hyde [12,13] to include electrostatic interactions and then by Vasut and Hyde [14] to simulate the formation of Coulomb crystals. BOX_TREE has proven to be an effective tool for modeling real time systems composed of large numbers of particles with specific interparticle interactions, especially complex (dusty) plasma systems. Recently, BOX_TREE has been used by Qiao and Hyde to investigate the dispersion properties of longitudinal and *in-plane* transverse DLW in 2D plasma crystals with the results agreeing well with previous experimental and theoretical research models [15,16].

*Email address: Truell_Hyde@Baylor.edu

The BOX_TREE code models such a system by first dividing the 3D box containing it into self-similar nested sub-boxes, where the box size is much greater than the radial mean excursions of the constituent particles. A tree code is incorporated into the BOX_TREE routine to allow it to deal with interparticle interactions. Since most such interactions can be determined by examining the multipole expansion of collections of particles in the sub-boxes, the code scales as $N \log N$ instead of N^2, resulting in greater CPU time efficiency. Different boundary conditions can be chosen with periodic boundary conditions, for example, being met using 26 ghost boxes [14]. Data files showing each particle's position and velocity are output for analysis after a user-defined time interval. The origin of the coordinate system is chosen to be at the center of the box.

In this work, the dust particles in the sheath region of the complex plasma are modeled as particles with a constant charge. The interparticle interactions considered include both gravitational and electrostatic forces. The interparticle electrostatic potential is assumed to be a 3D screened Coulomb repulsion or Yukawa potential with a user-specified Debye length. External forces considered include gravity and the electrostatic force. The electric field in the sheath region causing this electrostatic force has proven to depend linearly on particle height z [17,18]. Thus, the linear electrostatic field causing the electrostatic force is modeled as

$$E(z) = k\left(\frac{d}{2} - z\right), \tag{1}$$

where d is the height of the box and the linear coefficient $k = 8.3 \times 10^5$ kg/s^2. The neutral gas drag is included with a user-specified Epstein drag coefficient [19]. Other external forces, including ion drag and the thermophoretic force are neglected since they have been shown to be several orders of magnitude less than either the gravitational or the electrostatic force for the particle size examined [17,20]. For this research, the particle radius $r = 6.5\ \mu$m, the particle density $\rho = 1.51$ gm/cm^3, the particle charge $q = 24\,000e$, and the Epstein drag coefficient $\beta = 2.22$ s^{-1}. The boundary conditions in the XY directions are considered to be periodic since the box employed has a size much smaller than the size of the 2D plasma crystal in a typical experimental environment. The boundary condition on the Z direction is assumed to be a closed boundary condition with particles hitting the top or bottom boundaries of the box reflected under an elastic collision.

The crystallization of the complex (dusty) plasma is simulated via the formation of an ordered crystal from a random distribution of particles placed in the box subject to the condition that the system's center of mass should be located at the center of the box. The crystal forms approximately 50 s after the start of the simulation, by which time all the particles have been levitated and formed a horizontal 2D system with an equilibrium position $z_{eq} = 2.16$ mm. The state of the system was determined to be in a crystalline form (solid) using the pair correlation function and the lattice was found to be triangular (hexagonal) using the resulting Voronoi diagram [14]. The interparticle spacing a is obtained from the pair correlation function and $\kappa = a/\lambda_D$ is then calculated.

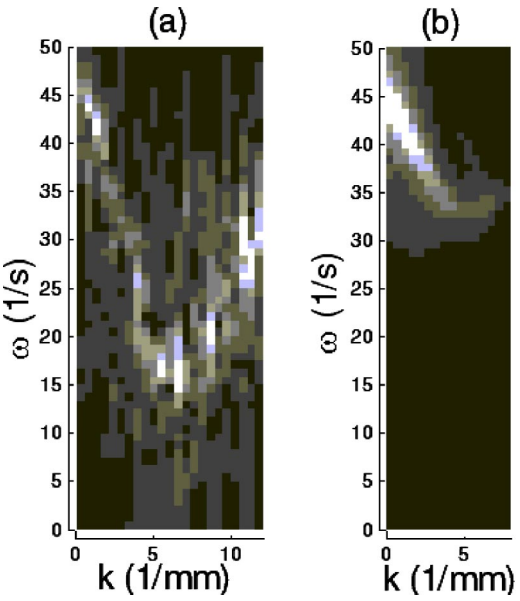

FIG. 1. The velocity matrix in ω-k space obtained from the numerical simulation for (a) $N = 590$ ($\kappa = 1.18$) and (b) $N = 400$ ($\kappa = 1.62$). The bright areas show the dispersion relations of the *out-of-plane* transverse DLW. The propagation direction is perpendicular to the prime translation vector.

Multiple 2D hexagonal Coulomb crystals with various κ values were formed by varying the particle number while keeping the box size and Debye length constant. In this research, the box is $15 \times 15 \times 15$ mm^3, the Debye length $\lambda_D = 570\ \mu$m, and the particle number N was varied between 300 and 590.

When $N > 570$, the vertical velocities of the thermal (spontaneous) motion of the particles in the Coulomb crystal are greater than 10^{-10} m/s, which is large enough that the dispersion relation of the DLW's can be obtained from an analysis of this spontaneous motion. The motion of the particles within the lattice is tracked for 10 s by choosing the data output time interval to be 0.01 s and collecting 1000 data files. Depending on the equilibrium particle positions, particles are divided into bins with their velocity averaged over each bin, yielding velocity data, which are dependent upon position. Combining data files, a velocity matrix depending on time t and position x can then be obtained. A double Fourier transformation of this matrix as given in Eq. (2) yields a matrix representing the particle velocity in k-ω space. The dispersion relation can then be observed in a graph drawn in k-ω space where particle velocities are differentiated using pixel intensity [Fig. 1(a)],

$$V_{k,\omega} = (2/TL) \int_0^T \int_0^L v(x,t) \times \exp[i(\omega t - kx)]\, dx\, dt, \tag{2}$$

where T is the time interval under estimation and L is the length of the box.

This numerical method can be employed to obtain dispersion relations for all wave modes [15,16] and any propagation direction. To obtain the dispersion relation for a wave with a specified propagation direction, the direction of the

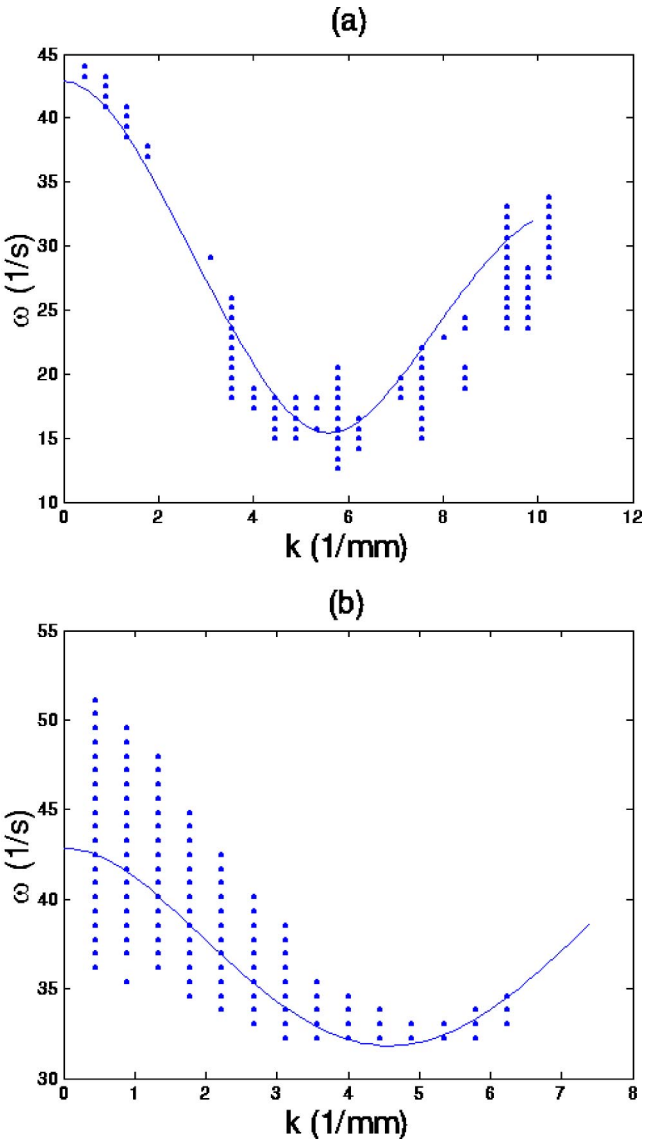

FIG. 2. The numerical (dots) and analytical (solid line) dispersion relation of the *out-of-plane* transverse DLW for (a) $N=590$ ($\kappa=1.18$) and (b) $N=400$ ($\kappa=1.62$). In both cases, the propagation direction is perpendicular to the prime translation vector.

bins is chosen to be perpendicular to the propagation direction. To obtain the dispersion relation of a given wave mode, the corresponding velocity components are chosen. In this research, the Z components of the velocities were chosen to study the *out-of-plane* transverse wave mode, which involves the vertical motion of the particles.

For $N<570$, the vertical velocities of the thermal (spontaneous) motion of the particles are on the order of 10^{-16} m/s and thus too small to be used to obtain the dispersion relation. For these situations, an excitation pulse was added to the code as a time-dependent external potential. Once data were collected, the dispersion relations were then obtained in the same manner as before [Fig. 1(b)].

III. ANALYTICAL METHOD

Assuming a hexagonal Coulomb crystal with Yukawa interparticle potential and grain levitation via the balanced

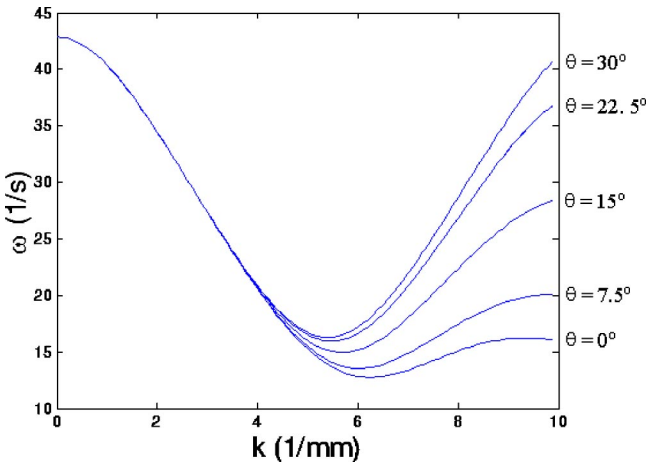

FIG. 3. The dispersion relation for the *out-of-plane* transverse DLW for $\kappa=1.18$ and various propagation directions. θ is defined as the angle between the propagation direction and the prime translation vector.

gravitational and linear electrostatic forces, the dispersion relation for the *out-of-plane* transverse DLW can be derived from the equation of motion

$$m\frac{d^2\xi^{jl}}{dt^2}+m\beta\frac{d\xi^{jl}}{dt}=-q\nabla_z\phi^{jl}-\mu\xi^{jl}. \tag{3}$$

In Eq. (3), ξ^{jl} represents the vertical deviation from the equilibrium position (x_0^{jl},y_0^{jl}) of the particle denoted by j, l in the lattice ($z_0^{jl}=0$ because all particles are in the same plane), m is the particle mass, q is the particle charge, β is the Epstein drag coefficient, and μ is the linear coefficient of the external electrostatic field. ϕ^{jl} is the electrostatic potential at position j,l and is given by the sum of the Yukawa potentials caused by each individual particle in the lattice except for the one located at position j,l.

Thus, the first term on the right-hand side of Eq. (3) can be written as

$$-q\nabla_z\phi^{jl}=\sum_{m,n\neq j,l}g_{mn}^{jl}(\xi^{jl}-\xi^{mn}), \tag{4}$$

where g_{mn}^{jl} is the spring constant between the dust particles located at jl and mn. A Taylor expansion of the Yukawa potential considering only small deviations in the Z direction yields

$$g_{mn}^{jl}=-\frac{q^2}{4\pi\varepsilon_0 r^3}\exp\left(-\frac{r}{\lambda_D}\right)\left(1+\frac{r}{\lambda_D}\right), \tag{5}$$

where r is the distance between (x_0^{jl},y_0^{jl}) and (x_0^{mn},y_0^{mn}). Employing the trial solution

$$\xi^{jl}=\xi_0\exp[i(kx_0^{jl}-\omega t)] \tag{6}$$

in Eq. (3) (when only propagation along the x direction is considered), the dispersion relation as given in Eq. (7) can easily be derived,

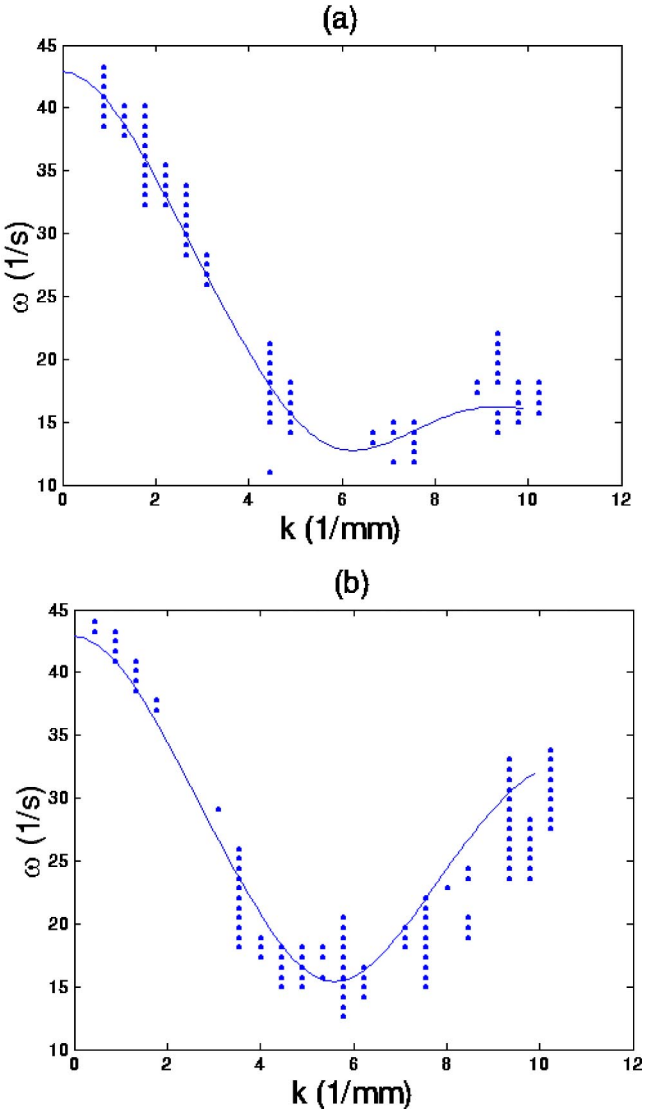

FIG. 4. The numerical (dots) and analytical (solid line) dispersion relation of the *out-of-plane* transverse DLW for $\kappa=1.18$ and propagation direction (a) parallel and (b) perpendicular to the prime translation vector.

$$\omega^2+i\beta\omega=\frac{\mu q}{m}-2\sum_{m.n\neq j,l}\frac{g_{mn}^{00}}{m}\sin^2\left(\frac{kx_0^{mn}}{2}\right). \qquad (7)$$

Again, as in Eq. (4), the summations in Eq. (7) are carried out over all particles in the lattice except particle j,l.

IV. RESULTS AND DISCUSSION

Upon examination, the vertical velocity of the particles was found to be sensitive to the particle number (or κ value) when N is around 580 (corresponding to a κ around 1.175). As N increases from 570 to 590, the average vertical velocity of the particles increases dramatically from the order of magnitude of 10^{-16} m/s to 10^{-6} m/s. For any $N<570$, the average vertical velocity is on the order of magnitude of 10^{-16} m/s. As mentioned before, this is why the dispersion relations can be obtained from the particle's thermal motion

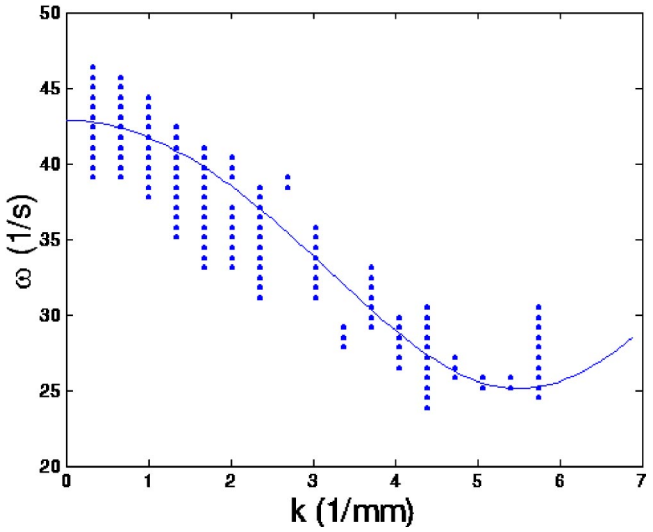

FIG. 5. The numerical (dots) and analytical (solid line) dispersion relation of the vertical DLW for a 1D string with $\kappa=1$ ($a=0.57$ mm).

when $N>570$ while for $N<570$ the lattice must be intentionally excited. For $N>590$, the particles no longer remain in the same plane and form a bilayer system. Discussion on this topic will be addressed in a subsequent article.

Figure 1 shows the dispersion relations for the *out-of-plane* transverse DLW obtained for $N=590$ ($\kappa=1.18$) and $N=400$ ($\kappa=1.62$). As can be seen, they are inverse optic-like dispersions, corresponding to a negative group velocity when k is lower than a critical value k_{critical} (long wavelength). As k passes k_{critical}, ω begins to increase with increasing k. Choosing data points with values above a specified level in Fig. 1 [15,16] and superimposing the analytical dispersion relation as expressed in Eq. (7), a solid fit can be seen in Fig. 2 between the numerical and analytical results for both κ values. The ω at $k=0\ \text{mm}^{-1}$ is the angular frequency of the single-particle oscillation in the sheath region ω_0. The negative group velocity of the wave for $k<k_{\text{critical}}$, which is equal to the slope of the inverse dispersion, depends on κ dramatically. For example, the group velocity v_g for $k<k_{\text{critical}}$ equals -7.135 mm/s for $\kappa=1.18$ and -3.624 mm/s for $\kappa=1.62$.

Figure 3 shows the analytical results of the dispersion relation for this wave mode with $\kappa=1.18$ and for representative propagation directions. In Fig. 4, a comparison between this analytical dispersion and the simulation results for two specified propagation directions, perpendicular and parallel to the prime translation vector, are given. Again they agree with each other for both directions. As can be seen, the negative group velocity for $k<k_{\text{critical}}$ is independent of propagation direction. However, the positive group velocity for $k>k_{\text{critical}}$ is sensitive to the propagation direction. For this case, it equals 5.162 mm/s for a propagation direction perpendicular to the prime translation vector and 1.714 mm/s for a propagation direction parallel to the prime translation vector.

It can also be seen from Figs. 2–4 that although k_{critical} depends on both κ and θ (with θ defined as the angle between the propagation direction and the prime translation

vector), it changes very little ($4.5\ \mathrm{mm}^{-1} < k_{\mathrm{critical}} < 6.5\ \mathrm{mm}^{-1}$) across all propagation directions and the range of κ investigated. For example, for $\kappa = 1.18$, $k_{\mathrm{critical}} = 5.5\ \mathrm{mm}^{-1}$ for $\theta = 30°$ and $k_{\mathrm{critical}} = 6.2\ \mathrm{mm}^{-1}$ for $\theta = 0°$ (Fig. 4). On the other hand, for $\theta = 30°$, $k_{\mathrm{critical}} = 4.6\ \mathrm{mm}^{-1}$ for $\kappa = 1.62$ and $k_{\mathrm{critical}} = 5.5\ \mathrm{mm}^{-1}$ for $\kappa = 1.18$ (Fig. 2).

Finally, a simulation was also run for a 1D string of particles having the same mass, charge, density, and Debye length as above. The system of particles was constrained to a 1D string by adding an external potential well on the y direction in the BOX_TREE code. As before, the dispersion relation for the *out-of-plane* transverse DLW was found and then compared with the analytical dispersion given by Vladimirov in [10], where they show a solid fit (Fig. 5). Comparing the dispersion relation for the 1D string with the 2D lattice, it can be seen that the negative group velocity for $k < k_{\mathrm{critical}}$ is much lower for the 1D string than it is for the 2D lattice given the same particle and environmental parameters. Figure 5 shows that the negative group velocity of the vertical DLW for a 1D string when $k < k_{\mathrm{critical}}$ and $\kappa = 1$ ($a = 0.57$ mm) is -8.536 mm/s.

All of the above is true even though k_{critical} for the 1D string equals $5.5\ \mathrm{mm}^{-1}$, as can be seen in Fig. 5, which is in the same range as k_{critical} for the 2D lattice investigated above ($4.5\ \mathrm{mm}^{-1} < k_{\mathrm{critical}} < 6.5\ \mathrm{mm}^{-1}$).

V. CONCLUSIONS

In summary, the dispersion properties of a novel low-frequency DLW mode in the 2D plasma crystal, the *out-of-plane* transverse DLW, have been examined. Using a numerical algorithm called BOX_TREE, the dispersion relation was shown to be an opticlike inverse dispersion for $k < k_{\mathrm{critical}}$ and a positive dispersion when $k > k_{\mathrm{critical}}$. The negative group velocity of the wave when $k < k_{\mathrm{critical}}$ depends on the κ value of the lattice and the positive group velocity for $k > k_{\mathrm{critical}}$ depends on the propagation direction of the wave. The value of k at which ω starts to increase, k_{critical}, depends on both κ and propagation direction, but changes very little for all propagation directions and the range of κ investigated.

An analytical method has also been used to derive the dispersion relations for the *out-of-plane* transverse DLW assuming a hexagonal 2D lattice and a Yukawa interparticle potential. These dispersion relations compare favorably with the simulation results.

Finally, the dispersion relation for a 1D string was obtained via a BOX_TREE simulation and shown to agree with the analytical result given by Vladimirov in [10]. Comparison shows that the *out-of-plane* transverse DLW in a 2D lattice when $k < k_{\mathrm{critical}}$ has a negative group velocity much larger than that for the 1D string, given the same particle and environmental parameters, although k_{critical} for both the 1D string and 2D lattice are in the same range ($4.5\ \mathrm{mm}^{-1} < k_{\mathrm{critical}} < 6.5\ \mathrm{mm}^{-1}$).

The results predicted in this research should be experimentally observable and could be used to determine the fundamental parameters of a complex (dusty) plasma such as the particle charge or Debye length. Corresponding experimental research is underway.

[1] J. H. Chu and I. Lin, Phys. Rev. Lett. **72**, 4009 (1994).
[2] Y. Hayashi and K. Tachibana, Jpn. J. Appl. Phys., Part 2 **33**, L804 (1994).
[3] H. Thomas *et al.*, Phys. Rev. Lett. **73**, 652–655 (1994).
[4] A. Homann *et al.*, Phys. Rev. E **56**, 7138 (1997).
[5] A. Homann *et al.*, Phys. Lett. A **242**, 173 (1998).
[6] S. Nunomura, D. Samsonov, and J. Goree, Phys. Rev. Lett. **84**, 5141 (2000).
[7] S. Nunomura *et al.*, Phys. Rev. E **65**, 066402 (2002).
[8] S. Nunomura *et al.*, Phys. Rev. Lett. **89**, 035001 (2002).
[9] X. Wang, A. Bhattacharjee, and S. Hu, Phys. Rev. Lett. **86**, 2569 (2001).
[10] S. V. Vladimirov, Physica A **315**, 222 (2002).
[11] D. Richardson, Mon. Not. R. Astron. Soc. **269**, 493–511 (1994).
[12] L. Matthews and T. Hyde, J. Phys. A **36**, 6207 (2003).
[13] L. Matthews and T. Hyde, Adv. Space Res. (to be published).
[14] J. Vasut and T. W. Hyde, IEEE Trans. Plasma Sci. **29**, 231–237 (2001).
[15] K. Qiao and T. Hyde, J. Phys. A **36**, 6109 (2003).
[16] K. Qiao and T. Hyde, Adv. Space Res. (to be published).
[17] E. B. Tomme, B. M. Annaratone, and J. E. Allen, Plasma Sources Sci. Technol. **9**, 87 (2000).
[18] E. B. Tomme *et al.*, Phys. Rev. Lett. **85**, 2518 (2000).
[19] P. S. Epstein, Phys. Rev. **23**, 710 (1924).
[20] T. G. Northrop and T. J. Birmingham, Planet. Space Sci. **38**, 319 (1990).